

# Experimental Over-The-Air Testing for Coexistence of 4G and A Spectrally Efficient Non-Orthogonal Signal

Tongyang Xu and Izzat Darwazeh

Department of Electronic and Electrical Engineering, University College London, London, UK

Email: t.xu@ee.ucl.ac.uk, i.darwazeh@ucl.ac.uk

**Abstract**—This work investigates several experimental validations for the bandwidth compressed multicarrier signal termed spectrally efficient frequency division multiplexing (SEFDM). The signal compresses bandwidth, therefore improved spectral efficiency, by packing sub-carriers closer. Unlike typical orthogonal frequency division multiplexing (OFDM) signals, SEFDM violates the orthogonality criterion, therefore self-created inter carrier interference (ICI) is introduced. In this work, to ameliorate the effect of interference, a method based on sub-carrier pulse shaping, targeting massive machine-type communication (mMTC), is developed and tested experimentally. Practical over-the-air testing of the proposal is operated on commercially developed software defined radio platforms. Results show that in the condition of coexistence scenario SEFDM can significantly reduce interference when used with existing long term evolution (LTE) signals leading to improved quality of service. The throughput of LTE signals is therefore improved from 49.92 Mbps to 63.21 Mbps. Additionally, the proposed pulse shaping Nyquist-SEFDM performs well in scenarios where the spectrum is limited and in fact it outperforms pulse shaped OFDM significantly, both in terms of bandwidth saving and throughput, which is boosted from 4.35 Mbps to 43.36 Mbps.

**Index Terms**—Experiment, multicarrier communications, spectral efficiency, OFDM, SEFDM, non-orthogonal, USRP, pulse shaping.

## I. INTRODUCTION

High throughput enhanced mobile broadband (eMBB) service is one requirement for future wireless networks. Multicarrier techniques are widely used in 4<sup>th</sup> generation (4G) [1] communication systems due to the high immunity against multipath fading with OFDM being the standardized technique in LTE and LTE-Advanced. OFDM improves spectral efficiency by overlapping sub-carriers orthogonally, such spectral efficiency can be further improved using SEFDM technique, initially proposed in 2003 [2], where sub-carriers are non-orthogonally overlapped. Thus, the spectral efficiency is higher than that of OFDM leading to improved throughput [3].

In future 5<sup>th</sup> generation (5G) [4] networks, a thousand-fold wireless traffic increase is predicted from 2020, emanating from over 50 billion connected devices [5]. Such massive device connection and communication, termed mMTC, will be associated with the continuously emerging internet of things (IoT). Currently, 80% of IoT applications require terminals with low power consumption, with an average battery life expectancy reaching 10 years [6]. However, in current 4G

networks, transceivers consume a large amount of energy due to complex signal processing. Future IoT devices have to be able to set up reliable services with simplified signal processing and extend their batteries lifetime.

To combine spectrum saving with overcoming the aforementioned challenges, one solution is to utilize sub-carrier pulse shaping [7] to cut out-of-band power leakage. This work will briefly introduce the SEFDM model and then describe the design concepts and experiments used to validate this solution.

## II. BANDWIDTH SAVING MODEL

The SEFDM signal consists of a stream of modulated SEFDM symbols each carrying  $N$  complex quadrature amplitude modulation (QAM) symbols. Each of the  $N$  complex symbols is modulated on one non-orthogonal sub-carrier. Therefore, the SEFDM signal can be expressed as

$$x(t) = \frac{1}{\sqrt{T}} \sum_{l=-\infty}^{\infty} \sum_{n=0}^{N-1} s_{l,n} \exp\left(\frac{j2\pi n\alpha(t-lT)}{T}\right) \quad (1)$$

where  $\alpha$  is the bandwidth compression factor defined as

$$\alpha = \Delta f T \quad (2)$$

$\Delta f$  denotes the frequency distance between adjacent sub-carriers,  $T$  is the period of one SEFDM symbol,  $\frac{1}{\sqrt{T}}$  is a scaling factor for the purpose of normalization,  $N$  is the number of sub-carriers and  $s_{l,n}$  is the complex QAM symbol modulated on the  $n^{\text{th}}$  sub-carrier in the  $l^{\text{th}}$  SEFDM symbol.  $\alpha$  determines bandwidth compressions and hence the percentage of bandwidth saving equals to  $(1 - \alpha) \times 100\%$ . For OFDM signals  $\alpha = 1$ , and  $\alpha < 1$  for SEFDM. Fig. 1 illustrates comparisons of the spectra of OFDM and SEFDM. It is clearly seen that due to non-orthogonal sub-carrier packing, SEFDM has a narrower bandwidth compared to OFDM given the same number of sub-carriers and the same modulation bandwidth per sub-carrier.

It is useful to represent the SEFDM signal in a discrete form for the purpose of signal analysis. A discrete signal is derived by sampling the first SEFDM symbol (take  $l=0$ ) at  $T/Q$  intervals where  $Q = \rho N$  and  $\rho \geq 1$  is the oversampling factor. The discrete SEFDM signal for  $k = [0, 1, \dots, Q - 1]$  is represented by

$$X[k] = \frac{1}{\sqrt{Q}} \sum_{n=0}^{N-1} s_n \exp\left(\frac{j2\pi nk\alpha}{Q}\right) \quad (3)$$

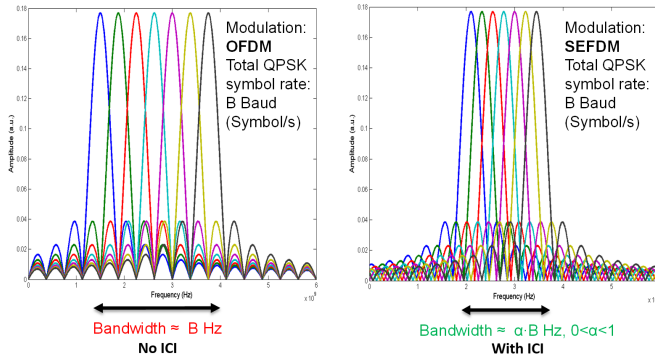


Figure 1. Spectra comparisons of OFDM and SEFDM.

where  $X[k]$  is the  $k^{\text{th}}$  time sample of the first symbol of  $x(t)$  in (1) and  $\frac{1}{\sqrt{Q}}$  is a scaling factor. Furthermore, the signal can be simply expressed in a matrix form as:

$$X = \mathbf{F}S \quad (4)$$

where  $X$  is a  $Q$ -dimensional vector of time samples of  $x(t)$  in (1),  $S$  is an  $N$ -dimensional vector of transmitted symbols and  $\mathbf{F}$  is a  $Q \times N$  sub-carrier matrix with elements equal to  $\exp(\frac{j2\pi nk\alpha}{Q})$ .

In a conventional OFDM system, signal generation can be realized straightforwardly by using a standard inverse fast Fourier transform (IFFT). However, due to the violation of the orthogonality property within SEFDM, the typical IFFT approach is not applicable. The direct way using equation (3) to address signal generation is too complex. In order to use the IFFT algorithm, two alternative algorithms are specially designed for SEFDM. Either using single IFFT or multiple IFFTs [8].

### III. INTER CARRIER INTERFERENCE

At the receiver,  $X$  as defined in (4) is contaminated by additive white Gaussian noise (AWGN)  $Z$ . The received signal is demodulated by correlating with the conjugate sub-carriers  $\mathbf{F}^*$ . The reception process is expressed as

$$R = \mathbf{F}^*X + \mathbf{F}^*Z = \mathbf{F}^*\mathbf{F}S + \mathbf{F}^*Z = \mathbf{C}S + Z_{\mathbf{F}^*} \quad (5)$$

where  $R$  is an  $N$ -dimensional vector of demodulated symbols or, in other words the received statistics,  $\mathbf{C}$  is an  $N \times N$  correlation matrix which is defined as  $\mathbf{C} = \mathbf{F}^*\mathbf{F}$ , where  $\mathbf{F}^*$  denotes the  $N \times Q$  conjugate sub-carrier matrix with elements equal to  $e^{-\frac{j2\pi nk\alpha}{Q}}$  for  $k = [0, 1, \dots, Q-1]$  and  $Z_{\mathbf{F}^*}$  is the AWGN correlated with the conjugate sub-carriers. Interference from non-orthogonal packed sub-carriers can be defined by using the correlation matrix  $\mathbf{C}$  [3], where elements in the matrix is expressed as

$$C(m, n) = \frac{1}{Q} \times \left\{ \begin{array}{ll} Q & , m = n \\ \frac{1 - e^{j2\pi\alpha(m-n)}}{1 - e^{\frac{j2\pi\alpha(m-n)}{Q}}} & , m \neq n \end{array} \right\}. \quad (6)$$

Effectively,  $C(m, n)$  is the interference on the  $m^{\text{th}}$  sub-carrier resulting from the  $n^{\text{th}}$  sub-carrier.

### IV. SUB-CARRIER PULSE SHAPING

In a real wireless communication scenario, radio spectrum is not always occupied. The unused portion of the radio spectrum is termed spectrum hole [9]. More specifically, the spectrum hole is defined that in a period of time, the licensed spectrum assigned to a primary user (PU) is not utilized. Meanwhile, the unlicensed radio resources are overly used due to open access. In order to balance the workload and further improve spectral efficiency, cognitive radio (CR) allows secondary users (SUs) to access spectrum holes that are unutilized by PUs at a particular time period. In a CR scenario, an SU firstly detects available spectrum holes and then adopts a proper modulation scheme, signal band and transmission power to minimize the interference to PUs. However, the use of rectangular pulses in typical OFDM systems results in high out-of-band power leakage and consequently in interference to adjacent frequency bands. Thus, a spectrally inefficient frequency gap has to be reserved as a protection gap between a PU and an SU to mitigate the interference. This compromises the overall spectral efficiency.

Recently, a spectrally efficient concept, termed generalized frequency division multiplexing (GFDM) [10], employing a root raised cosine (RRC) pulse shaping filter for each sub-carrier, demonstrated significant reduction of out-of-band power leakage, when applied to the multicarrier system. Work in [10] has verified that with the assistance of a successive interference cancellation scheme, GFDM can achieve the same BER performance as that of the rectangular pulse shaped OFDM. Another filtering based system is filterbank based multicarrier (FBMC) [11], which copes with the ICI challenge by using offset-QAM (OQAM) [12] modulation scheme, where the real and imaginary parts of QAM complex symbols are separated by delaying the imaginary branch of a QAM symbol by half of symbol duration before passing through a pulse shaping filter. Thus, no successive interference cancellation is needed. It should be noted that contrary to SEFDM, the sub-carrier spacing of the GFDM and FBMC systems is still equal to the symbol rate, in other words, both systems assume  $\alpha=1$ . Since the out-of-band power is significantly suppressed in GFDM and FBMC, it would be spectrally advantageous to reduce the sub-carrier spacing below the symbol rate and reduce the out-of-band power at the same time. Therefore, the motivation for the implementation of pulse shaped Nyquist-SEFDM [7] is to create a spectrally efficient (i.e. bandwidth saving) system with reduced out-of-band power.

The spectra of rectangular shaped OFDM/SEFDM and RRC shaped OFDM/SEFDM are shown Fig. 2. It is apparent that the RRC shaped spectrum has a much lower out-of-band power leakage. The out-of-band power of SEFDM in Fig. 2(c) is approximately 18 dB below the spectral peak. Using RRC pulse shaping, in Fig. 2(d), such out-of-band power leakage is reduced by a further 27 dB. This indicates that SEFDM is better than OFDM in both bandwidth saving and the out-of-band power suppression.

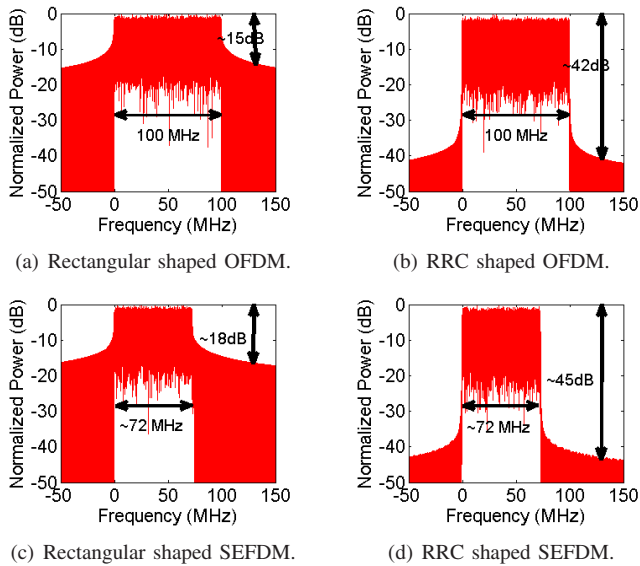


Figure 2. Bandwidth saving and out-of-band power reduction comparisons for various signals. Using the same number of sub-carriers, the bandwidth is compressed by 28% in SEFDM systems, the roll-off factor of the RRC filter is  $\beta=0.5$ . This figure is reused from our previous work in [7].

## V. OVER-THE-AIR TESTING USING SOFTWARE DEFINED RADIO DEVICES

Experimental work discussed below is based on two independent universal software radio peripheral (USRP) RIO 2953R platforms [13]. The actual setup, shown in Fig. 3, is designed to test the coexistence of SEFDM signal and LTE signal. LTE framework [14] is used as a tool to evaluate the proposed waveform. In this case, two USRPs, one implements SEFDM transceiver while the other one implements the LTE framework transceiver, are used to transmit over the air asynchronously operated.

The main benefit of this testbed is that the entire SEFDM system can be jointly implemented in software and hardware. LabVIEW is the software tool that implements part of the functions aligning with the FPGA integrated in the USRP RIO platform. A computer is connected to the USRP RIO and is used to generate the digital signals to be transmitted and to process received digital signals. The analogue signal processing is integrated in the USRP RIO device using 14 bit analog-to-digital convertor (ADC) and 16 bit digital-to-analogue convertor (DAC) clocked at 120MS/s. The wireless signal transmission link is set up between USRP RF0 out port and RF1 in port via two omnidirectional antennas on each USRP with a 8 dBi peak gain in the azimuth plane. Two antennas are arranged with a line-of-sight (LOS) link and the spacing between the two antennas is 12cm and the antennas are placed 0.8 m above the floor. Two sets of Tx/Rx antennas are spaced approximately 14cm. Thus, possible interference would occur on RX ports of both USRPs. Host A is for user defined SEFDM/OFDM signal generation and reception. The measured results include spectrum and interference effect.

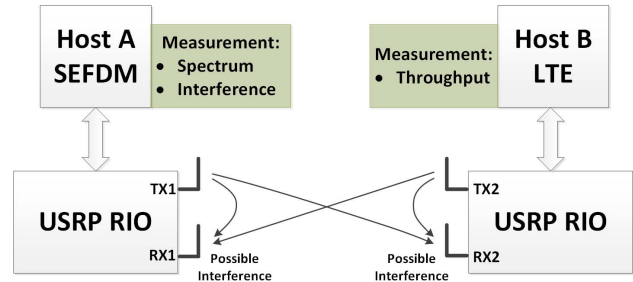
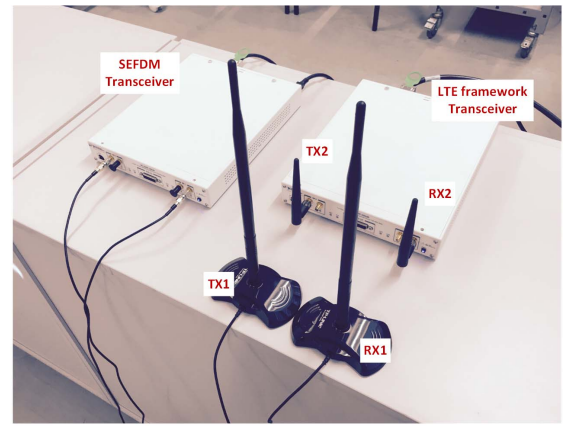


Figure 3. Double SEFDM/OFDM testbeds setup using USRP RIO for the evaluations of coexistence of SEFDM and LTE signals.

Host B is for LTE standardized signal transmission and reception. The physical USRP setup is shown in Fig. 3. Antennas are deployed in this experiment for the testing of a realistic LOS wireless scenario. For multipath fading scenarios, we have experimentally tested SEFDM signals in work [3].

This work is focused on coexistence performance with existing 4G LTE (i.e. 20MHz channel bandwidth) signals. Therefore, the detection of our designed SEFDM signal, which introduces extra complexity and power consumption, is skipped. Many efficient SEFDM signal detection schemes have been developed either based on uncoded [15][16] or coded [17][18] for various size systems.

Table I  
EXPERIMENTAL TESTBED SPECIFICATIONS FOR NON-PULSE SHAPED SYSTEMS

Parameters	OFDM	SEFDM
Central carrier frequency (GHz)	2.412	2.412
Modulation scheme	4QAM	4QAM
Sampling rate (MHz)	45	45
FFT size	1024	1024
Number of data sub-carriers	176	176
Bandwidth compression factor	1	0.6
Sub-carrier spacing (kHz)	44	26.4
Data bandwidth (MHz)	7.73	4.64
Data rate (Mbps)	15.46	15.46

Screenshots illustrating the coexistence performance are provided in Fig. 4 where two scenarios are considered. In the first scenario (top part of Fig. 4), OFDM (i.e.  $\alpha=1$ ) and LTE



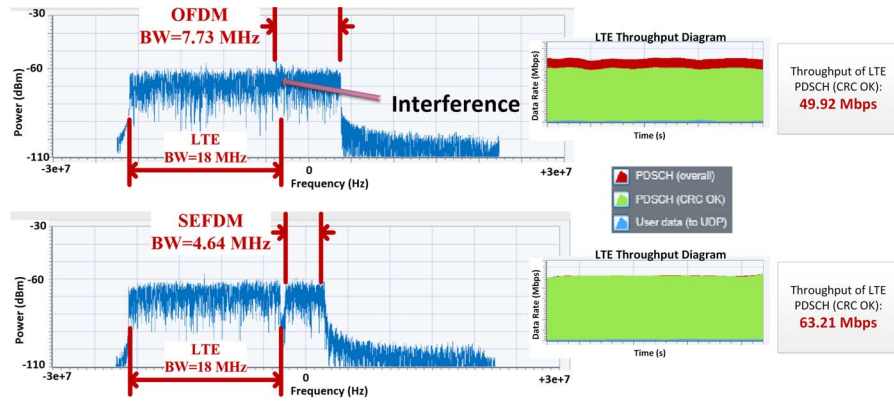


Figure 4. Coexistence of SEFDM/OFDM and LTE signals in a bandwidth limited scenario shown at baseband frequency.

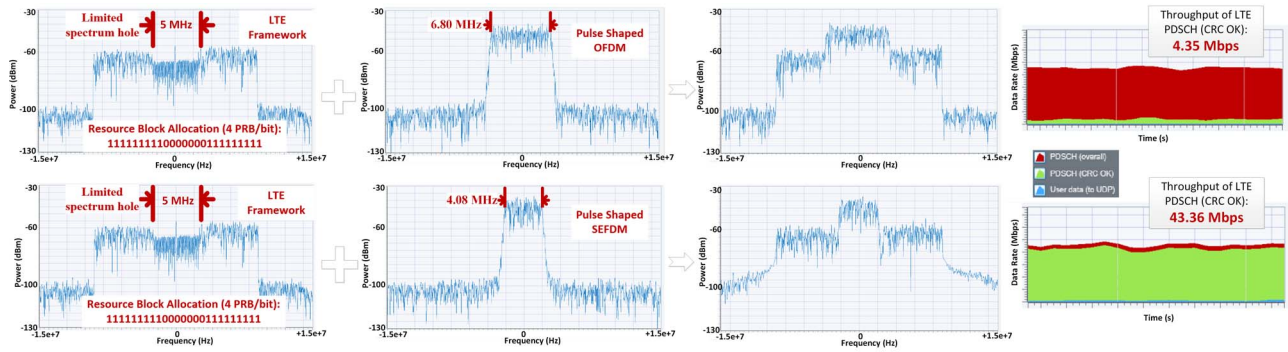


Figure 5. Coexistence of pulse shaped SEFDM/OFDM and LTE signals in a limited spectrum hole shown at baseband frequency.

signals are transmitted and evaluated. The OFDM signal is configured based on Table I, with associated spectrum clearly showing interference occurring due to the spectral overlap of the two signals. The LTE signal is degraded and this can be observed from the LTE throughput diagram where the red region in the figure indicates lower throughput measured through observation of the cyclic redundancy check (CRC) field of LTE data transmitted on the physical downlink shared channel (PDSCH) (overall) throughput and PDSCH (CRC OK) throughput. It indicates that the PDSCH transmission is not always correct. For this case throughput of the PDSCH (CRC OK) is measured to be 49.79 Mbps. Our proposed solution to use SEFDM signals which, due to its reduced bandwidth, can avoid spectral overlap. The results are shown in the lower part of Fig. 4. The new SEFDM signal specifications are presented in Table I. Due to the compressed bandwidth of SEFDM signals, a protection guard band is reserved between the LTE spectrum and the SEFDM spectrum. In the LTE throughput diagram, it is apparent that the received PDSCH transmission is almost free (no red region is observed) with a measured throughput of PDSCH (CRC OK), equals to 63.21 Mbps. This means that using SEFDM not only saves spectrum but improves throughput of an adjacent LTE system by a factor of 27%.

As mentioned in section IV, pulse shaping can cut the

Table II  
EXPERIMENTAL TESTBED SPECIFICATIONS FOR PULSE SHAPED SYSTEMS

Parameters	OFDM	SEFDM
Central carrier frequency (GHz)	2.4	2.4
Modulation scheme	4QAM	4QAM
Sampling rate (MHz)	30	30
FFT size	128	128
Number of data sub-carriers	29	29
Roll-off factors	1	1
Bandwidth compression factor	1	0.6
Data bandwidth (MHz)	6.80	4.08
Data rate (Mbps)	13.60	13.60

out-of-band power leakage leading to reduced interference to adjacent signals. Pulse shaping for SEFDM and GFDM has been conceptually studied in [7] and [10], respectively. Reusing the testbed in Fig. 3, the Nyquist-SEFDM and GFDM can be evaluated using antennas in a realistic wireless environment. It can be demonstrated that Nyquist-SEFDM can achieve the same benefits of GFDM [10] and will add additional interference avoidance benefit. Fig. 5 shows the performance of the coexistence of Nyquist-SEFDM/GFDM and LTE signals, with their system specifications shown in Table II.

A sufficient spectrum hole indicates a wide enough notch that can be occupied by an additional signal band. To eval-

uate the benefit of Nyquist-SEFDM over Nyquist-OFDM (or GFDM), the LTE signal was modified to narrow the spectrum hole, indicating limited spectrum hole as shown in Fig. 5. The notch width maybe easily changed in the experimental setup. In the first scenario, the sharp edge of the pulse shaped OFDM spectrum is due to the pulse shaping applied to each sub-carrier. The spectrum hole is emulated by deactivating some physical resource blocks (PRBs) of an LTE spectrum. The combination of the two signal bands leads to making new spectrum available. It is clearly seen that the Nyquist-OFDM spectrum overlaps the LTE one with interference introduced. The throughput, observed from the LTE throughput diagram, drops to 4.35 Mbps. This indicates that Nyquist-OFDM (or GFDM) has significant interference on the LTE signal even with reduced out-of-band leakage in a bandwidth limited scenario. In the second scenario, Nyquist-SEFDM shows its benefits. Although the spectrum notch is narrow, due to the bandwidth compression characteristic, interference can be avoided in the combined spectrum. Thus the LTE PDSCH (CRC OK) throughput is 43.36 Mbps, which is much higher than the one achieved in the first scenario by nearly one order of magnitude. Therefore, the benefits of using SEFDM in either rectangular shaped or RRC shaped systems are clear and have been summarized in Table III. In both coexistence scenarios, SEFDM signals boost the LTE signal throughput greatly due to the interference avoidance coming from SEFDM bandwidth compression.

Table III  
COMPARISONS OF EXPERIMENTAL LTE SIGNAL THROUGHPUT

Parameters	OFDM	SEFDM
Traditional systems in Fig. 4 (Mbps)	49.92	63.21
Pulse shaped systems in Fig. 5 (Mbps)	4.35	43.36

## VI. CONCLUSIONS

SEFDM is a bandwidth compressed waveform while Nyquist-SEFDM is a new waveform that can save bandwidth and reduce out-of-band interference simultaneously. Thus, these waveforms meet the requirement of eMBB and mMTC scenarios. Several experiments based on the use of software defined radio equipment (national instruments USRP), where designed and reported in the paper. Based on the experimental results, it is concluded that SEFDM signals can bring throughput benefits in two USRPs signal coexistence scenario. The throughput of LTE signals is therefore improved by 26.6%. Moreover, the signal coexistence scenario indicates that the pulse shaped Nyquist-SEFDM signal significantly outperforms Nyquist-OFDM signal in terms of throughput performance, being improved by approximately 896.8%, in bandwidth limited scenarios.

## VII. ACKNOWLEDGEMENT

This work was part funded by the Engineering and Physical Sciences Research Council (EPSRC) “Discovery to Use

Impact Acceleration” award for the development of a pre-commercialization 5G transceiver prototype and part funded by the University College London (UCL) Faculty of Engineering Sciences Scholarship (Dean’s Scholarship). The work was also supported by National Instruments and by a generous donation of the LTE FPGA core through the Xilinx University Program (XUP).

## REFERENCES

- [1] 3GPP TR 36.912 v.13.0.0, “Feasibility study for further advancements for E-UTRA (LTE-Advanced),” Rel. 13, Dec. 2015.
- [2] M. Rodrigues and I. Darwazeh, “A spectrally efficient frequency division multiplexing based communications system,” in *Proc. 8th Int. OFDM Workshop*, Hamburg, 2003, pp. 48–49.
- [3] T. Xu and I. Darwazeh, “Transmission experiment of bandwidth compressed carrier aggregation in a realistic fading channel,” *IEEE Transactions on Vehicular Technology*, vol. 66, no. 5, pp. 4087–4097, May 2017.
- [4] J. Andrews, S. Buzzi, W. Choi, S. Hanly, A. Lozano, A. Soong, and J. Zhang, “What will 5G be?” *Selected Areas in Communications, IEEE Journal on*, vol. 32, no. 6, pp. 1065–1082, June 2014.
- [5] H. A. U. Mustafa, M. A. Imran, M. Z. Shakir, A. Imran, and R. Tafazolli, “Separation framework: An enabler for cooperative and D2D communication for future 5G networks,” *IEEE Communications Surveys Tutorials*, vol. 18, no. 1, pp. 419–445, Firstquarter 2016.
- [6] Huawei Technologies Co., Ltd., “NB-IOT, Accelerating Cellular IOT,” <http://www.huawei.com/minisite/hwmbbf15/en/nb-iot-accelerating-cellular-iot.html>, 2015.
- [7] T. Xu and I. Darwazeh, “Nyquist-SEFDM: Pulse shaped multicarrier communication with sub-carrier spacing below the symbol rate,” in *2016 10th International Symposium on Communication Systems, Networks and Digital Signal Processing (CSNDSP)*, July 2016, pp. 1–6.
- [8] P. Whatmough, M. Perrett, S. Isam, and I. Darwazeh, “VLSI architecture for a reconfigurable spectrally efficient FDM baseband transmitter,” *Circuits and Systems I: Regular Papers, IEEE Transactions on*, vol. 59, no. 5, pp. 1107–1118, May 2012.
- [9] R. Tandra, S. M. Mishra, and A. Sahai, “What is a spectrum hole and what does it take to recognize one?” *Proceedings of the IEEE*, vol. 97, no. 5, pp. 824–848, May 2009.
- [10] R. Datta, N. Michailow, M. Lentmaier, and G. Fettweis, “GFDM interference cancellation for flexible cognitive radio PHY design,” in *Vehicular Technology Conference (VTC Fall), 2012 IEEE*, Sept 2012, pp. 1–5.
- [11] B. Farhang-Boroujeny, “OFDM versus filter bank multicarrier,” *Signal Processing Magazine, IEEE*, vol. 28, no. 3, pp. 92–112, May 2011.
- [12] P. Siohan, C. Siclet, and N. Lacaille, “Analysis and design of OFDM/OQAM systems based on filterbank theory,” *Signal Processing, IEEE Transactions on*, vol. 50, no. 5, pp. 1170–1183, May 2002.
- [13] National Instruments, “USRP-RIO-2953R,” <http://sine.ni.com/nips/cds/view/p/lang/en/nid/213005>.
- [14] —, “LabVIEW Communications LTE Application Framework,” <http://sine.ni.com/nips/cds/view/p/lang/en/nid/213083>.
- [15] T. Xu, R. C. Grammenos, F. Marvasti, and I. Darwazeh, “An improved fixed sphere decoder employing soft decision for the detection of non-orthogonal signals,” *Communications Letters, IEEE*, vol. 17, no. 10, pp. 1964–1967, October 2013.
- [16] T. Xu and I. Darwazeh, “Multi-Band reduced complexity spectrally efficient FDM systems,” in *9th IEEE/IET International Symposium on Communication Systems, Networks & Digital Signal Processing 2014 (CSNDSP14)*, Manchester, United Kingdom, Jul. 2014, pp. 904–909.
- [17] —, “A soft detector for spectrally efficient systems with non-orthogonal overlapped sub-carriers,” *Communications Letters, IEEE*, vol. 18, no. 10, pp. 1847–1850, Oct 2014.
- [18] H. Ghannam and I. Darwazeh, “Comparison of turbo decoder and Turbo equalizer for spectrally efficient FDM system,” in *2016 10th International Symposium on Communication Systems, Networks and Digital Signal Processing (CSNDSP)*, July 2016, pp. 1–6.